Influence of *Meso* Substituents on Electronic States of (Oxoferryl)porphyrin π-Cation Radicals

K. Jayaraj,[†] J. Terner,*[,‡] A. Gold,*[,†] D. A. Roberts,[†] R. N. Austin,[†,⊥] D. Mandon,[§] R. Weiss,*[,§] E. Bill,[∥] M. Müther,[∥] and A. X. Trautwein*[,∥]

Department of Environmental Sciences and Engineering, The University of North Carolina at Chapel Hill, Chapel Hill, North Carolina 27599, Department of Chemistry, Virginia Commonwealth University, Richmond, Virginia 23284, Institut LeBel, Université Louis Pasteur, 67070 Strasbourg, France, and Institut für Physik, Medizinische Universität zu Lübeck, Lübeck, Germany

Received August 10, 1995[⊗]

A series of (oxoferryl)porphyrin π-cation radicals generated from porphyrins substituted at the *meso* positions with highly electron-withdrawing aryl groups has been characterized: tetrakis-5,10,15,20-(2,6-dichlorophenyl)-, 5-(2-chloro-6-nitrophenyl)-10,15,20-tris(2,6-dichlorophenyl)-, and 5-(2,6-dinitrophenyl)-10,15,20-tris(2,6-dichlorophenyl)porphyrins (porphyrins **1**−**3**, respectively). The physical−chemical properties of the oxidized complexes of **1**−**3** are compared to those of two (oxoferryl)porphyrin π-cation radical complexes substituted with electron-releasing aryl groups: tetramesitylporphyrin (TMP) and 2-iodotetramesitylporphyrin (2-iodoTMP). While all of the complexes examined show close correspondance in a number of spectroscopic parameters, some significant differences were observed. In contrast to observations for the oxidized complexes of TMP and 2-iodoTMP, the resonance Raman marker bands ν_2 and ν_{11}, which are indicators of symmetry state of porphyrin π-cation radicals of **1**−**3**, do not show the expected downfrequency shifts for oxidation to compound I analogs in a_{2u} symmetry states. The upfield hyperfine NMR shifts of the pyrrole β-proton signals of the compound I analogs of **1**−**3** are much larger than those for TMP and 2-iodoTMP. These data may be explained by admixture of some a_{1u} character into the ground state of radical cations of **1**−**3**, consistent with the hypothesis that electron-withdrawing *meso* substituents lower the energy of the a_{2u} molecular orbital, favoring an a_{1u} admixture.

Introduction

Physicochemical investigations involving the low temperature generation and stabilization of oxidized forms of model synthetic iron porphyrins[1−11] have contributed toward understanding the active site mechanisms of heme enzymes and proteins which participate in a wide variety of metabolic processes in living systems. High-valent iron porphyrins have been either identified or proposed as crucial intermediates in the reactions of peroxidases, catalases, cytochromes P-450, cytochrome oxidase, and other heme-based enzymes found in animals and plants.[12−16]

The best known of the physiological high valent-hemes are the sequential intermediates of the protoheme-containing peroxidases and related catalases.[12−14] These intermediates, commonly designated as compounds I and II, are respectively two and one oxidation equivalents above the resting ferric state. Mössbauer and resonance Raman spectroscopy have provided evidence for an oxoferryl unit in the compound I and compound II type intermediates. The additional oxidation equivalent in compound I resides on the porphyrin ring, resulting in an (oxoferryl)porphyrin π-cation radical electronic structure. Formation of the macrocycle π-cation radical involves electron abstraction from one of two nearly degenerate porphyrin frontier molecular orbitals corresponding to the a_{1u} and a_{2u} molecular orbitals in the notation of D_{4h} symmetry.[17] Since protohemes are prone to oxidative attack at the unprotected *meso*-positions, model studies have employed the more robust *meso*-tetraarylporphyrins in which such attack is hindered. An important distinction between protoheme and *meso*-tetraaryl-substituted porphyrins of model systems is the ordering of the frontier molecular orbitals; for protohemes, the a_{1u}-like molecular orbital is higher in energy than the a_{2u}-like orbital, while this order is

[†] The University of North Carolina at Chapel Hill.
[‡] Virginia Commonwealth University.
[§] Université Louis Pasteur.
[∥] Medizinische Universität zu Lübeck.
[⊥] Current address, Department of Chemistry, Bates College, Lewiston, ME 04240.

[⊗] Abstract published in *Advance ACS Abstracts,* February 1, 1996.

(1) Boso, B.; Lang, G.; McMurry, T. J.; Groves, J. T. *J. Chem. Phys.* **1983**, *79*, 1122−1126.
(2) Groves, J. T.; Haushalter, R. C.; Nakamura, M.; Nemo, T.; Evans, B. J. *J. Am. Chem. Soc.* **1981**, *103*, 2884−2886.
(3) Groves, J. T.; Myers, R. S. *J. Am. Chem. Soc.* **1983**, *105*, 5791−5796.
(4) Groves, J. T.; Nemo, T. E. *J. Am. Chem. Soc.* **1983**, *105*, 6243−6248.
(5) Bill, E.; Ding, X. Q.; Bominaar, E. L.; Trautwein, A. X.; Winkler, H.; Mandon, D.; Weiss, R.; Gold, A.; Jayaraj, K.; Hatfield, W. E.; Kirk, M. L. *Eur. J. Biochem.* **1990**, *188*, 665−672.
(6) Bill, E.; Bominaar, E. L.; Ding, X. Q.; Trautwein, A. X.; Winkler, H.; Mandon, D.; Weiss, R.; Gold, A.; Jayaraj, K.; Tony, G. E. *Hyperfine Interactions* **1990**, *58*, 2343−2348.
(7) Mandon, D.; Weiss, R.; Jayaraj, K.; Gold, A.; Terner, J.; Bill, E.; Trautwein, A. X. *Inorg. Chem.* **1992**, *31*, 4404−4409.
(8) Hashimoto, S.; Mizutani, Y.; Tatsuno, Y.; Kitagawa, T. *J. Am. Chem. Soc.* **1991**, *113*, 6542−6549.
(9) Kincaid, J. R.; Schneider, A. J.; Paeng, K.-J. *J. Am. Chem. Soc.* **1989**, *111*, 735−737.
(10) Proniewicz, L. M.; Paeng, I. R.; Nakamoto, K. *J. Am. Chem. Soc.* **1991**, *113*, 3294−3303.
(11) Fujii, H. *J. Am. Chem. Soc.* **1993**, *115*, 4641−4648.
(12) Andersson, L. A.; Dawson, J. H. *Struct. Bonding* **1990**, *74*, 1−40.
(13) Hawkins, B. K. and Dawson, J. H. in *Frontiers in Biotransformation*; Ruckpaul, K., Rein, H., Eds.; Akademie Verlag: Berlin, 1992; Vol. 7, pp 216−278.
(14) Dawson, J. H. *Science* **1988**, *240*, 433−439.
(15) McMurry, T. J.; Groves, J. T. In *Cytochrome P-450: Structure, Mechanism and Biochemistry*; Ortiz de Montellano, P. R., Ed.; Plenum Press: New York, 1986; pp 1−28.
(16) Marnett, L. J.; Weller, P.; Battista, J. R. In *Cytochrome P-450: Structure, Mechanism and Biochemistry*; Ortiz de Montellano, P. R., Ed.; Plenum Press: New York, 1986; pp 29−76.
(17) Dolphin, D.; Felton, R. H. *Acc. Chem. Res.* **1974**, *7*, 26−32.

0020-1669/96/1335-1632$12.00/0

reversed for the *meso*-substituted porphyrins.[18−22] Thus, the ground state of protoheme π-cation radicals is expected to have a_{1u} symmetry, while that of *meso* substituted porphyrin π-cation radicals is expected to have a_{2u} symmetry. Recent theoretical calculations on the relative ordering of the frontier molecular orbitals have suggested that peripheral substituents, metal ions and axial ligands[21−24] may influence the $a_{1u}-a_{2u}$ energy separation. In particular, substitution of electron-withdrawing groups at porphyrin *meso* carbons is predicted to exert a significantly stabilizing influence on the a_{2u} porphyrin molecular orbital, creating a favorable situation for admixture of a_{1u} character into the A_{2u} state.[21,22] Because of the different nodal structure and electron spin density distribution of the frontier orbitals,[25,26] the character of the half-occupied molecular orbital should, in principle, be identifiable by spectroscopic methods. To gain insight into the nature of the oxidized states of both model compounds and enzymes, we have investigated the possibility of such tuning of electronic state. Using an array of spectroscopic techniques, we have characterized a series of three (oxoferryl)porphyrin π-cation radicals generated from complexes of porphyrins substituted at the *meso* positions with highly electron-withdrawing aryl groups: tetrakis-5,10,15,20-(2,6-dichlorophenyl)-; 5-(2-chloro-6-nitrophenyl)-10,15,20-tris-(2,6-dichlorophenyl)- and 5-(2,6-dinitrophenyl)-10,15,20-tris-(2,6-dichlorophenyl)porphyrin (porphyrins **1**−**3**, respectively). The physical−chemical properties of the (oxoferryl)porphyrin π-cation radical complexes of **1**−**3** are compared to those of two (oxoferryl)porphyrin π-cation radical complexes substituted with electron-releasing *meso*-aryl groups: tetramesitylporphyrin (TMP), the most extensively studied compound I analog, and 2-iodotetramesitylporphyrin (2-iodoTMP). Substitution of a bulky iodine atom at a pyrrole β position allows perturbation of ligand symmetry to be investigated in the well-studied TMP framework. Resonance Raman data are correlated with other spectroscopic data: ^{1}H NMR, EPR, and Mössbauer. Of particular interest is the behavior of the resonance Raman marker bands ν_2 and ν_{11}, which should be sensitive to symmetry state admixture in the porphyrin radical cations.

Experimental Section

General Methods. The procedure employed for synthesis of substituted tetraarylporphyrins conformed in general to the published Lewis acid catalyzed condensation of aryl aldehydes with pyrrole.[27,28] The asymmetric metal-free porphyrin bases 5-(2-chloro-6-nitrophenyl)-10,15,20-tris(2,6-dichlorophenyl)porphyrin (**2**) and 5-(2,6-dinitrophenyl)-10,15,20-tris(2,6- dichlorophenyl) porphyrin (**3**) were obtained by condensing pyrrole with a 3:1 ratio of 2,6-dichlorobenzaldehyde and the appropriate nitrobenzaldehyde derivative. Yields for the Lewis acid-catalyzed condensation with 2,6-dinitrobenzaldehyde were low and inconsistent, and the target compound was difficult to purify. Problems with the use of dinitrobenzaldehyde have been noted by Lindsey[27] and others.[29] 2-Iodotetramesitylporphyrin was obtained by condensing mesitaldehyde with a 2:1 mixture of pyrrole:3-iodopyrrole synthesized by a published procedure.[30]

Metalations were accomplished according to published methods.[31] For Mössbauer studies, porphyrins were metalated with $^{57}FeCl_2$ obtained by stirring ^{57}Fe foil in refluxing 1:1 HCl:methanol under an inert atmosphere, as described elsewhere.[7]

The trifluoromethanesulfonate (triflate) complexes of **1**−**3** were obtained from the corresponding chloro complexes by metathesis with silver triflate according to published procedures.[32] Ferric complexes of mono- and dinitroporphyrins **2** and **3** have not yet been reported and were characterized by ^{1}H NMR, UV−vis, and FAB MS. EPR and magnetic Mössbauer spectra have been reported[33] for the compound I analog of 2-iodoTMP; however, ^{1}H NMR, UV−vis, and FAB MS have not been reported for the ferric complex and are given below.

Chloro(5-(2-chloro-6-nitrophenyl)-10,15,20-tris(2,6-dichlorophenyl)porphinato)iron(III), [Fe^{III} (2)]$^+$Cl$^-$. ^{1}H NMR (400 MHz, chloroform-*d*): 8.2 (asymmetric s, 4H, phenyl *p*-H), 12.7 (bs, 3H, 10,-15,20-phenyl *m*-H), 12.8 (bs, 1H, 5-phenyl *m*-H3), 13.4 (bs, 1H, 5-phenyl *m*-H5), 14.0 (bs, 3H, 10,15,20-phenyl *m*-H), 14.4 (bs, 1H, 5-phenyl *m*-H3), 14.8 (bs, 1H, 5-phenyl *m*-H5), 82.0 (bs, 8H, py-H) ppm; atropisomerism is indicated by asymmetry in *m*-H and *p*-H resonances of phenyl substituents. UV−vis (methylene chloride) [λ_{max} ($\epsilon \times 10^{-3}$)]: 360 (35.22), 415 (70.58), 505 (8.26), 576 (2.47), 641 (2.53) nm. FAB MS (*p*-nitrobenzyl alcohol matrix) cluster at (M − axial chloride) with highest peaks of equal intensities at *m*/*z* 953, 955 consistent with the pattern required for seven chlorine atoms.

Chloro(5-(2,6-dinitrophenyl)-10,15,20-tris(2,6-dichlorophenyl)-porphinato)iron(III), [Fe^{III} (3)]$^+$Cl$^-$. ^{1}H NMR (500 MHz, chloroform-*d*): 8.2 (bs, 3H, 10,15,20-phenyl *p*-H), 8.4 (s, 1H, 5-phenyl *p*-H), 12.6 (bs, 1H, 15-phenyl *m*-H), 12.8 (bs, 2H, 10,20-phenyl *m*-H), 14.0 (bs, 2H, 10,20-phenyl *m*-H), 14.3 (bs, 1H, 15-phenyl *m*-H), 15.2 (bs, 1H, 5-phenyl *m*-H), 17.3 (bs, 1H, 5-phenyl *m*-H), 80.3 (br s, 6H, py-H), 82.3 (br s, 2H, py-H) ppm. UV−vis (chloroform) [λ_{max}($\epsilon \times 10^{-3}$)]: 360 (51.36), 421 (105.0), 507 (15.15), 639 (6.67) nm. FAB MS (*p*-nitrobenzyl alcohol matrix): cluster at (M − axial chloride) with highest peak at *m*/*z* 964, base cluster *m*/*z* 934 (M − NO) consistent with the pattern required for six chlorine atoms.

Chloro(5,10,15,20-tetramesityl-2-iodoporphinato)iron(III), [Fe^{III} (2-iodoTMP)]$^+$Cl$^-$. ^{1}H NMR (400 MHz, chloroform-*d*): 2.9 (bs, 18H, 10,15,20-phenyl *o*-CH_3), 4 (bs, 12H, phenyl *p*-CH_3), 6.3 (bs, 6H, 5-phenyl *o*-CH_3), 14.2 (bs, 4H, *m*-H), 15.7 (bd, 4H, *m*-H), 79.0 m, 6H, py-H), 91.2 (bs, 1H, py-H) ppm. UV−vis (methylene chloride) [λ_{max} ($\epsilon \times 10^{-3}$)]: 379 (46), 420 (88.5), 510 (14), 583 (8) nm. FAB MS (dithioerythritol/dithiothreitol matrix): M^+ at *m*/*z* 962.

Oxidized Iron Complexes. The (oxoferryl)porphyrin π-cation radicals ([Fe^{IV}=O(P)]$^+$, P = porphyrinate dianion) were generated in methylene chloride or butyronitrile at −80 °C by the addition of *m*-chloroperoxybenzoic acid (*m*CPBA; two mass equivalents, approximately 8-fold molar excess) in methanol-d_4 (to give a methanol-d_4 concentration of ∼10%), according to published procedures.[7] Oxoferryl complexes of **1** and **2** ([Fe^{IV} = O(P)]) were generated by oxidizing the appropriate hydroxoiron(III) complex with *m*CPBA under the same conditions used for generation of the compound I analogs.

Specific techniques for generating Mössbauer, EPR and NMR samples as well as the instrumentation have been described.[7] For resonance Raman spectroscopy, (oxoferryl)porphyrins and (oxoferryl)-porphyrin π-cation radicals were generated at −80 °C in a cryostatted spinning cell.[7]

Results

UV−Visible Spectra. On treatment with *m*CPBA at −80 °C in methylene chloride−methanol-d_4 or butyronitrile−

(18) Czernuszewicz, R. S.; Macor, K. A.; Li, X.-Y.; Kincaid, J. R.; Spiro, T. G. *J. Am. Chem. Soc.* **1989**, *111*, 3860−3869.
(19) Oertling, W. A.; Salehi, A.; Chang, C. K.; Babcock, G. T. *J. Phys. Chem.* **1989**, *93*, 1311−1319.
(20) Hanson, L. K.; Chang, C. K.; Davis, M. S.; Fajer, J. *J. Am. Chem. Soc.* **1981**, *103*, 663−670.
(21) Spellane, P. J.; Gouterman, M.; Antepas, A.; Kim, S.; Liu, Y. C. *Inorg. Chem.* **1980**, *19*, 386−391.
(22) Skillman, A. G.; Collins, J. R.; Loew, G. H. *J. Am. Chem. Soc.* **1992**, *114*, 9538−9544.
(23) Binstead, R. A.; Crossley, M. J.; Hush, N. S. *Inorg. Chem.* **1991**, *30*, 1259−1264.
(24) Shelnutt, J. A.; Ortiz, V. *J. Phys. Chem.* **1985**, *89*, 4733−4739.
(25) Prendergast, K.; Spiro, T. G. *J. Phys. Chem.* **1991**, *95*, 9728−9736.
(26) Macor, K. A.; Czernuszewicz, R. S.; Spiro, T. G. *Inorg. Chem.* **1990**, *29*, 1996−2000.
(27) Lindsey, J. S.; Wagner, R. *J. Org. Chem.* **1989**, *54*, 828−936.
(28) Wagner, R. W.; Lawerence, D. S.; Lindsey, J. S. *Tetrahedron Lett.* **1987**, *27*, 3069−3070.
(29) Quintana, C. A.; Assink, R. A.; Shelnutt, J. A. *Inorg. Chem.* **1989**, *28*, 3421−3425.
(30) Bray, B.; Mathies, P.; Naef, R.; Solas, D.; Tidwell, T.; Artis, D.; Muchowski, J. *J. Org. Chem.* **1990**, *55*, 6317−6328.
(31) Adler, A. D.; Longo, F. R.; Kampas, R.; Kim, J. *J. Inorg. Nucl. Chem.* **1970**, *32*, 2443−2445.
(32) Gismelseed, A.; Bominaar, E. L.; Bill, E.; Trautwein, A. X.; Winkler, H.; Nasri, H.; Doppelt, P.; Mandon, D.; Fischer, J.; Weiss, R. *Inorg. Chem.* **1990**, *29*, 2741−2749.
(33) Müther, M.; Bill, E.; Trautwein, A. X.; Mandon, D.; Weiss, R.; Gold, A.; Jayaraj, K.; Austin, R. N. *Hyperfine Interact.* **1994**, *91*, 803−808.

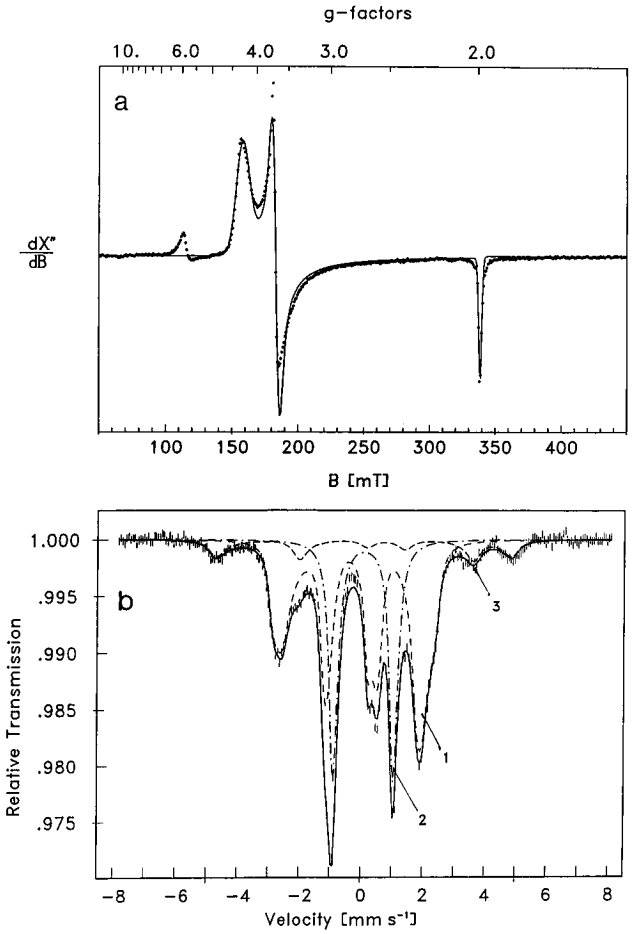

Figure 1. (a) X-Band EPR spectrum of $[Fe^{IV}{=}O(\mathbf{2})]^+$ at 10 K in methylene chloride/methanol-d_4. Conditions: microwave frequency 9.4 GHz, microwave power 20 μW, modulation frequency 100 kHz, and modulation amplitude 2 mT. The solid line is a simulation with effective g values g_{eff} = (3.68, 4.26, 1.990), which are derived from the spin Hamiltonian parameters from part b, discussed below, and Gaussian line widths Γ = (5, 11, 3) mT. (b) Mössbauer spectrum of $[Fe^{IV}{=}O(\mathbf{2})]^+$ in butyronitrile/methanol-d_4, recorded at 4.2 K in a field of 20 mT applied perpendicular to the direction of γ-irradiation. Subspectrum 1 (62% relative abundance) is a spin Hamiltonian simulation with D = 25 cm^{-1} (preliminary value; any value in the range 20−35 cm^{-1} is consistent with experimental data if J_o is allowed to be covariant), E/D = 0.06, J_o/D = 1.7, $J_{anisotropic}$ = (1, 2, −3) cm^{-1}, $g_{Fe(IV)}$ = (2.10, 2.12, 1.995). The Heisenberg term was $-S{\cdot}J{\cdot}S'$ with $J = J_o(\mathbf{1}) - J_{anisotropic}$, S = 1 for Fe(IV) and S' = $^1/_2$ for the porphyrin radical. The Mössbauer parameters were A = (−25.4, −25.1, −10) T, δ = 0.063 mm s^{-1}, ΔE_q = 1.45 mm s^{-1}. Subspectrum 2 (29% relative abundance) is a corresponding simulation for an oxoferryl species without a porphyrin radical, and subspectrum 3 (9% relative abundance) represents ferric starting material. The solid line represents the sum of the three subspectra.

Table 1. UV−Vis Data for (Oxoferryl)porphyrin π-Cation Radicals in Methylene Chloride/Methanol-d_4, −80 °C

porphyrin	λ_{max}, nm ($\epsilon \times 10^{-3}$)
1	391 (79.90), 678 (10.70)
2	393 (59.80), 682 (4.60)
3	396 (28.75), 687 (3.96)

methanol-d_4 solution, the ferric triflate complexes of **1**−**3** gave the bright green color characteristic of (oxoferryl)porphyrin π-cation radicals. The UV−visible data are tabulated (Table 1) and are typical of spectra observed for other model compound I analogs[2,5,7−9,11] derived from *meso*-tetraarylporphyrin complexes, having a low-intensity, broadened Soret band at ∼400 nm and a band in the visible region between 660 and 690 nm. The UV−visible spectra show no indication of contamination by one-electron reduced (oxoferryl)porphyrins, which have characteristic bands in the visible region at 550 nm and an intense Soret band[34,35] at 420 nm. Because of the low molar absorptivity and blue shift of the (oxoferryl)porphyrin π-cation radical Soret band and the absence of any bands in the vicinity of 550 nm, UV−visible spectroscopy is highly sensitive to the presence of oxoferryl impurities.

Table 2. ^{1}H NMR Shifts (ppm) for (Oxoferryl)porphyrin π-Cation Radicals from Complexes of **1**−**3**, 2-iodoTMP, and TMP at 500 MHz (Methylene-d_2 Chloride:Methanol-d_4 9:1, − 65 °C)

porphyrin	pyrrole-H	phenyl *m*-H
1	−61.2	31.7
2	−55.5(sh), −54.8, −54.3(sh)	37.6, 37.0, 36.5, 36.2, 35.0, 34.7, 34.5, 34.2, 33.0
3	−54.9, −54.3, −51.4	37.1, 36.9, 34.1, 33.9, 33.8, 33.7
2-iodoTMP	−24, −27(br sh).	72.9, 71.1, 70.9, 70.1, 70.0, 69.0, 68.7
TMP	−27.6	70.6

Mössbauer and EPR Spectroscopy. The Mössbauer and EPR spectra of the oxoferryl tetrakis(2,6-dichlorophenyl)-porphyrin π-cation radical, along with a detailed analysis of the data, have been reported.[5,7] The spectra are similar in appearance to those of the compound I analog generated from iron tetramesitylporphyrin (TMP) complexes and are interpreted as being indicative of an (oxoferryl)porphyrin π-cation radical structure in which the ferryl iron and the porphyrin radical are exchange-coupled to give a quartet ground state. The features of the EPR and Mössbauer spectra of the compound I analogs generated from complexes of **2** and **3**, in which one or both chlorine atoms of one phenyl group have been replaced by NO_2, closely resemble those of **1**. The EPR traces at 10 K (e.g., Figure 1a) show a rhombic signal with lines at $g^{eff}_{\perp} \sim 4$ and $g^{eff}_{||} \sim 2$. The Mössbauer spectrum of the compound I derivative of **2** in Figure 1b is representative of data obtained at 4.2 K in a weak magnetic field (200 G) oriented perpendicular to the direction of γ-irradiation. Resolution of the spectrum into a four line pattern can be ascribed to perturbation of the quadrupole doublet of low-spin ferryl iron by the magnetic field of the porphyrin π-cation radical. The Mössbauer and EPR parameters of the (oxoferryl)porphyrin π-cation radicals of **2** and **3** were estimated by spectral simulations using a spin Hamiltonian that explicitly included a Heisenberg exchange term to describe exchange coupling.[7] Traces of fitted EPR and Mössbauer spectra of the mononitro-substituted complex in Figure 1a,b are representative of the results obtained by this process. The simulations confirm that the oxidized complexes of **2** and **3** can also be adequately described as parallel-coupled (oxoferryl)porphyrin π-cation radicals. The EPR and Mössbauer spectra demonstrate that compound I analogs of the catalytically active halogenated porphyrins can be efficiently generated.

^{1}H NMR. The ^{1}H NMR spectra of the (oxoferryl)porphyrin π-cation radicals generated from complexes of **1**−**3** are displayed in Figure 2 and the chemical shifts and assignments of resonances presented in Table 2. The pyrrole and phenyl *m*-H resonances appear substantially upfield from the corresponding proton resonances of TMP[11] and show the expected C_s symmetry for complexes of **2** and **3**. In addition, atropisomerism in the relative orientations of the oxo-ligand and nitro group in the 2-chloro-6-nitrophenyl complex is indicated by resolution of two sets of phenyl *m*-proton signals for the nitro-substituted aryl ring (Figure 2, panel b). The phenyl *p*-H resonances have not been definitively identified. Resonances at ∼14 ppm and 25−32 ppm in the NMR spectra of the oxidized complexes are

(34) Gold, A.; Jayaraj, K.; Doppelt, P.; Weiss, R.; Chottard, G.; Bill, E.; Ding, X.; Trautwein, A. X. *J. Am. Chem. Soc.* **1988**, *110*, 5756−5761.
(35) Chin, D. H.; Balch, A. L. *J. Am. Chem. Soc.* **1980**, *102*, 1446−1448.

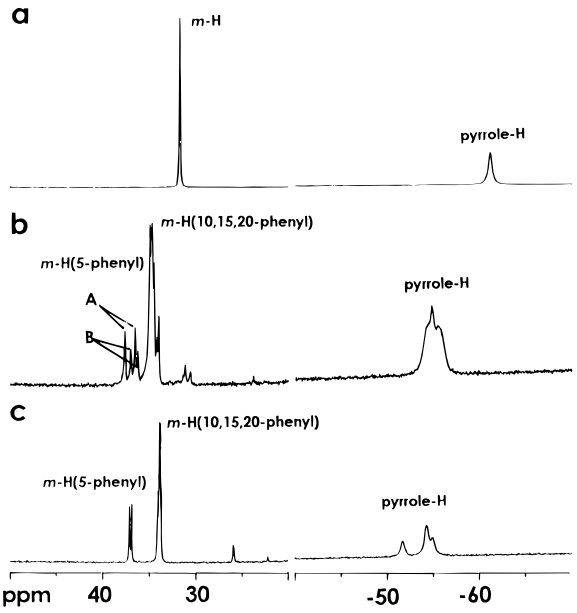

Figure 2. ^{1}H NMR traces (500 MHz, methylene-d_2 chloride/methanol-d_4, −65 °C) of (a) [Fe^{IV}═O(**1**)]$^+$, (b) [Fe^{IV}═O(**2**)]$^+$ and (c) [Fe^{IV}═O(**3**)]$^+$. Resonance assignments are indicated on traces and accurate hyperfine shifts of assigned resonances are given in Table 2. Atropisomers of [Fe^{IV}═O(**2**)]$^+$ are evident in the resolution of two sets of *m*-H resonances for the nitro-substituted phenyl ring designated A, B in trace b.

Table 3. Resonance Raman Skeletal Mode Frequencies (cm^{-1}) for Iron Complexes of Tetrakis(2,6-dichlorophenyl)porphyrin

mode	p	iron(III) triflate	iron(III) hydroxo	Fe^{IV}═O	[Fe^{IV}═O(P)]$^+$
ν_{phenyl}	p	1578	1585	1585	
ν_{10}	dp				1593
ν_{37}	p				1585
ν_2	p	1558	1563	1568	1565
ν_{19}	ap		1527		
ν_{11}	dp	1490	1499	1498	1515
ν_{28}	dp				1469
ν_3	p	1465	1472	1468	1458
$2\nu_{phenyl}$	p	1427	1436	1434	
CH_2Cl_2	dp	1423	1423	1423	1422
ν_4	p	1364	1367	1370	1318
ν_{29}	dp	1361			1362
ν_{21}			1339		
ν_{12}	dp	1284	1291	1291	1286
	dp	1257	1260		1261
ν_1	p	1233	1238	1239	1245

tentatively assigned to oxoferryl impurities arising from transient warming during transfer of the NMR sample tubes from the cold bath to NMR probe.

Resonance Raman. In Tables 3−5, the bands of the (oxoferryl)porphyrin π-cation radicals of **1**−**3** and corresponding lower oxidation-state complexes in the high frequency region (1200−1700 cm^{-1}) under Soret excitation (406.7 nm) are identified. Band assignments for complexes of the neutral porphyrin ligands are based on assignments for (metallotetraphenyl)porphyrins,[36] and no unusual features or frequency shifts are observed. Bands in the radical cation spectra have been correlated with published assignments for the oxoferryltetramesitylporphyrin π-cation radical and other (metallotetraphenyl)porphyrin π-cation radical complexes[18,19,26] through variation of band intensities in the polarized spectra. The highest phenyl mode, normally found at 1600 cm^{-1} for the tetraphenylporphyrins, is assigned to a lower frequency band at 1580 cm^{-1},

(36) Li, X.-Y.; Czernuscewicz, R. S.; Kincaid, J. R.; Su, Y. O.; Spiro, T. G. *J. Phys. Chem.* **1990**, *94*, 31−47.

Table 4. Resonance Raman Frequencies (cm^{-1}) for Skeletal Modes of Iron Complexes of 5-(2-Chloro-6-nitrophenyl)-10,15,20-tris-(2,6-dichlorophenyl)porphyrin

mode	p	iron(III) triflate	iron(III) hydroxo	Fe^{IV}═O	[Fe^{IV}═O(P)]$^+$
ν_{phenyl}	p	1583	1580	1581	
ν_{10}	dp			1585	1598
ν_2	p	1562	1559	1567	1566
ν_{NO}		1550			1552
ν_{19}	ap		1525		
ν_{11}	dp	1493	1497	1501	1515
ν_{28}	dp		1485	1492	1471
ν_3	p	1468	1468	1467	1458
$2\nu_{phenyl}$	p	1432	1433	1433	
CH_2Cl_2	dp	1423	1423	1424	1423
ν_4	p	1367	1364	1367	1323
ν_{29}	dp	1366			1368
ν_{12}	dp	1290	1285	1290	
	dp	1262	1257		
ν_1	p	1236	1235	1236	1248

Table 5. Resonance Raman Frequencies (cm^{-1}) for Skeketal Modes of Iron Complexes of 5-(2,6-Dinitrophenyl)-10,15,20-Tris-(2,6-dichlorophenyl)porphyrin

mode	p	iron(III) triflate	[Fe^{IV}═O(P)]$^+$
ν_{phenyl}	p	1582	1589
ν_{10}	dp	1567	
ν_2	p	1559	1560
ν_{NO}			1548
		1525	
ν_1	dp	1491	
ν_{28}		1471	
ν_3	p	1467	
$2\nu_{phenyl}$	p	1433	
CH_2Cl_2	dp	1424	1424
ν_4	p	1365	1327
ν_{29}	dp		1364
ν_{12}	dp	1287	1289
	dp	1260	
ν_1	p	1237	1248

corresponding to the mode in dichlorobenzene.[37] The phenyl mode upshifts to 1590 cm^{-1} upon porphyrin π-cation radical formation. Vibrations of the nitro groups are identified following the assignments of Shelnutt et al.[38] Even at −80 °C the lifetimes of the (oxoferryl)porphyrin π-cation radicals are relatively short, and ferryl contaminants normally appear within 5 to 10 min. Since the porphyrin π-cation radical resonance Raman spectra are characterized by broadened frequencies, ferryl contaminants can readily be recognized by their narrow band widths, as well as by laser power and time dependence. Figures 3 and 4 illustrate the traces of the polarized spectra of ferric, oxoferryl and (oxoferryl)porphyrin π-cation radical complexes of **1** and **2** for purposes of comparison. It is evident by comparing Figure 3b with Figure 3d and Figure 4b with Figure 4d that the (oxoferryl)porphyrin π-cation radicals are not contaminated with a reduced complex.

Figures 3d and 4d and Tables 4 and 5 show that the ν_2 band of (oxoferryl)porphyrin π-cation radicals of **1** and **2** shifts only a few wave numbers relative to the oxoferryl complexes. Tables 3−5 show that ν_2 of the compound I analogs of all three porphyrins moves *up* in frequency relative to the ferric triflate complexes. For the (oxoferryl)porphyrin π-cation radicals generated from **1** and **2**, ν_{11} shifts to higher frequency by more than 15 cm^{-1} compared to any of the corresponding ferric or oxoferryl complexes of neutral porphyrin ligands. Because of

(37) Dollish, F. R.; Fateley, W. G.; Bentley, F. F. *Characteristic Raman Frequencies of Organic Compounds*; Wiley: New York, 1974; pp 175−179, 376−382.

(38) Anderson, K. K.; Hobbs, J. D.; Luo, L.; Stanley, K. D.; Quirke, J. M. E.; Shelnutt, J. A. *J. Am. Chem. Soc.* **1993**, *115*, 12346−12352.

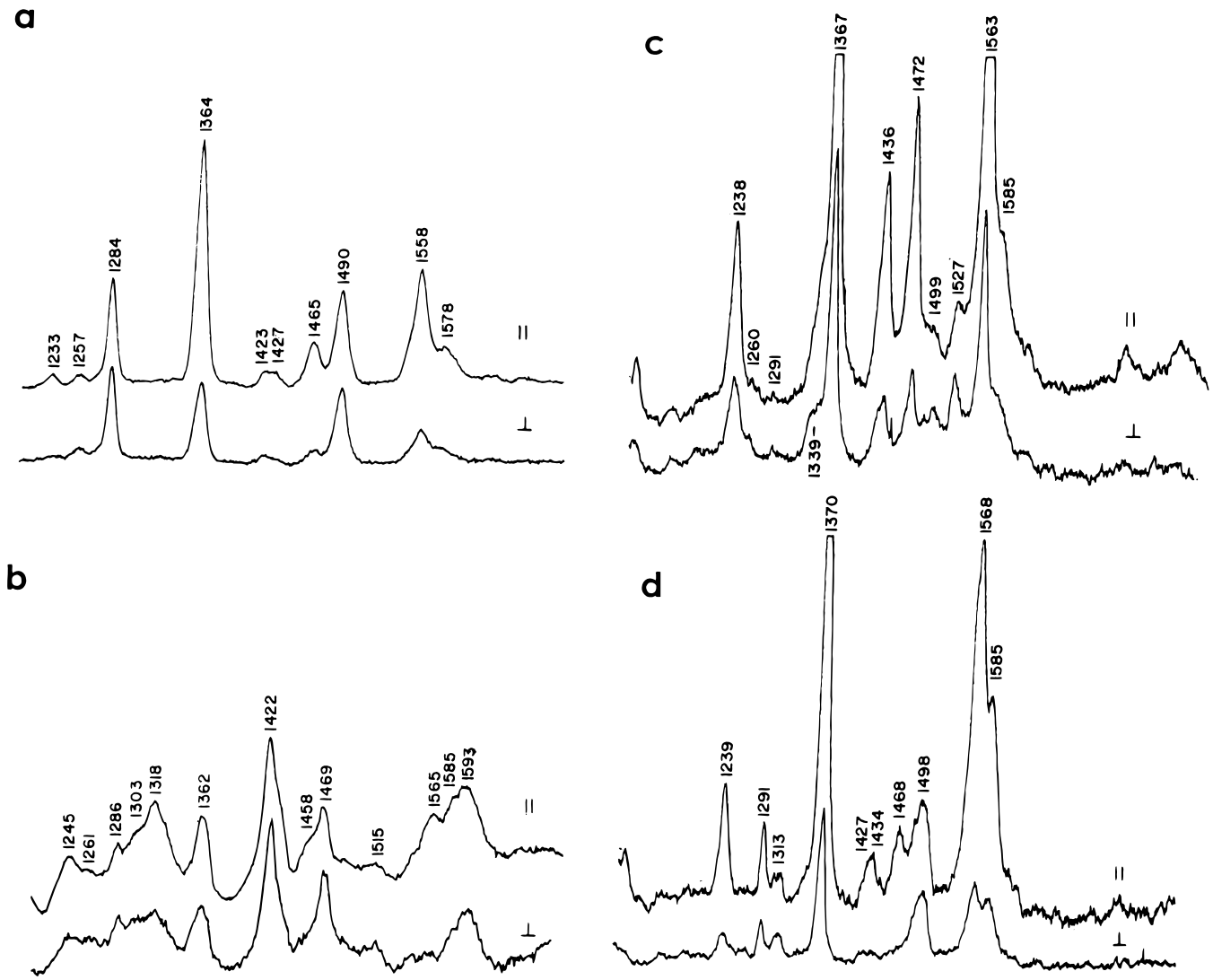

Figure 3. Resonance Raman spectra with 406.7 nm excitation (15 mW) for the 1250−1600 cm^{-1} region at −80° for (a) (tetrakis(2,6-dichlorophenyl)-porphinato)iron(III) triflate in methylene chloride; (b) same compound as in part a but reacted with an 8-fold molar excess of *m*CPBA in methanol-d_4 forming the (oxoferryl)porphyrin π-cation radical; (c) (tetrakis(2,6-dichlorophenyl)porphinato)iron(III) hydroxide; (d) same compound as in part c but reacted with an 8-fold molar excess of *m*CPBA forming the oxoferryl complex.

fluorescence interference, ν_{11} could not be resolved in the spectrum of the compound I analog of **3**.

The resonance Raman spectrum of the compound I analog from **1** contains a resolved band assigned to the E_u mode ν_{37}. The complex generated from **2** appears to contain ν_{37} on the low frequency edge of ν_{10}. In both the neutral and compound I analogs of **2** and **3**, broadened bands at ∼1550 cm^{-1} could contain contributions from both the asymmetric NO_2 stretch and E_u mode ν_{38}. Activation of the E_u modes is an indication of the lowering of D_{4h} symmetry.[38,39]

A substantial down-frequency shift of ν_4 is observed in the (oxoferryl)porphyrin π-cation radicals from **1**−**3** revealing the presence of ν_{29} at ∼1365 cm^{-1}. In the spectra of the oxidized complexes **2** and **3**, the band in the region of ν_{29} could also contain a contribution from the strong symmetric NO_2 stretch.[38]

We observed the Fe−O stretching frequency of the compound I analogs of **1** and **2** under resonance Raman conditions and confirmed the assignment of $\nu_{Fe=O}$ by ^{18}O labeling (Figure 5). Under our reaction conditions (presence of methanol-d_4), the Fe−O stretch for both complexes appears near 830 cm^{-1}.

Supporting resonance Raman studies were carried out on the (oxoferryl)porphyrin π-cation radicals generated from TMP and 2-iodoTMP, in which the 4-fold symmetry of TMP has been perturbed by substitution of a bulky iodine atom at a pyrrole β position. The results are presented in Figures 6 and 7 and Tables 6 and 7. The phenyl modes appear at >1600 cm^{-1} and undergo little change in frequency on porphyrin ring oxidation. For both the TMP and 2-iodoTMP-derived compound I analogs, ν_2 shows substantial down-frequency shifts (Figures 6 and 7; Tables 6 and 7). The ν_{11} band of the compound I analogs generated from ferric TMP and 2-iodoTMP shift only slightly from the positions of the corresponding neutral ferric complexes, in contrast to the behavior described above for **1** and **2**. As in the case of **1**−**3**, a large downshift of ν_4 on oxidation reveals ν_{29}.

Discussion

Initial investigations of metalloporphyrin π-cation radicals sought to correlate electronic spectra with symmetry state. Recent work has demonstrated the importance of complementary spectroscopic data[40] to substantiate such assignments. In the present study, compound I analogs generated from **1**−**3** were characterized by UV−visible, EPR, Mössbauer, NMR and resonance Raman spectroscopy.

In resonance Raman spectra, the formation of porphyrin π-cation radicals results in band shifts which have been

(39) Hobb., J. D.; Majumder, S. A.; Luo, L.; Sickelsmith, H. A.; Quirke, J. M. E.; Mdeforth, C. J.; Smith K. M.; Shelnutt, J. A. *J. Am. Chem. Soc.* **1994**, *116*, 3261−3270.

(40) Erler, B. S.; Scholz, W. F.; Lee, Y. J.; Scheidt, W. R.; Reed, C. A. *J. Am. Chem. Soc.* **1987**, *109*, 2644−2652.

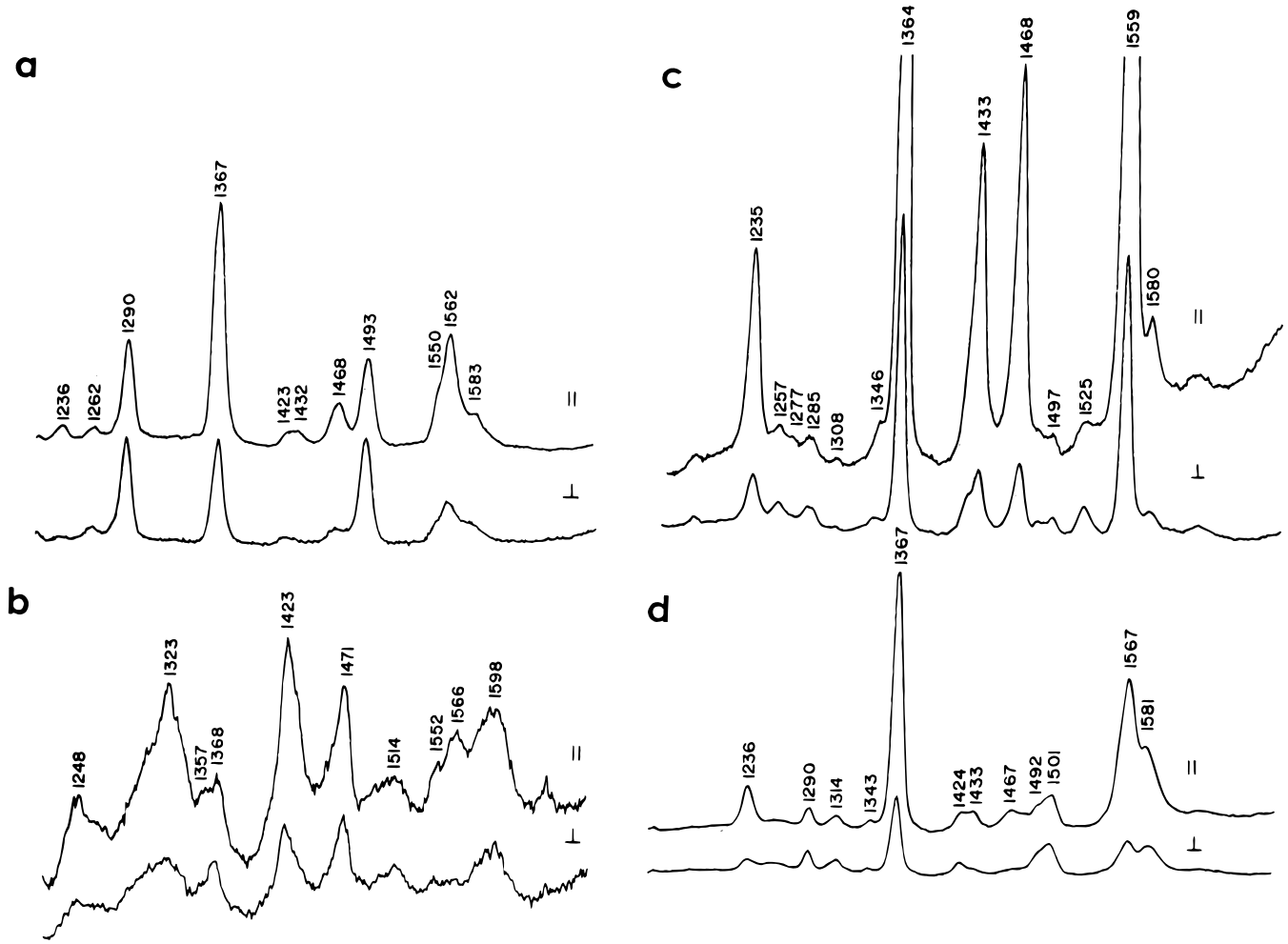

Figure 4. Resonance Raman spectra as in Figure 3 but for the complexes of 5-(2-chloro-6-nitrophenyl)-10,15,20-tris(2,6-dichlorophenyl)porphyrin.

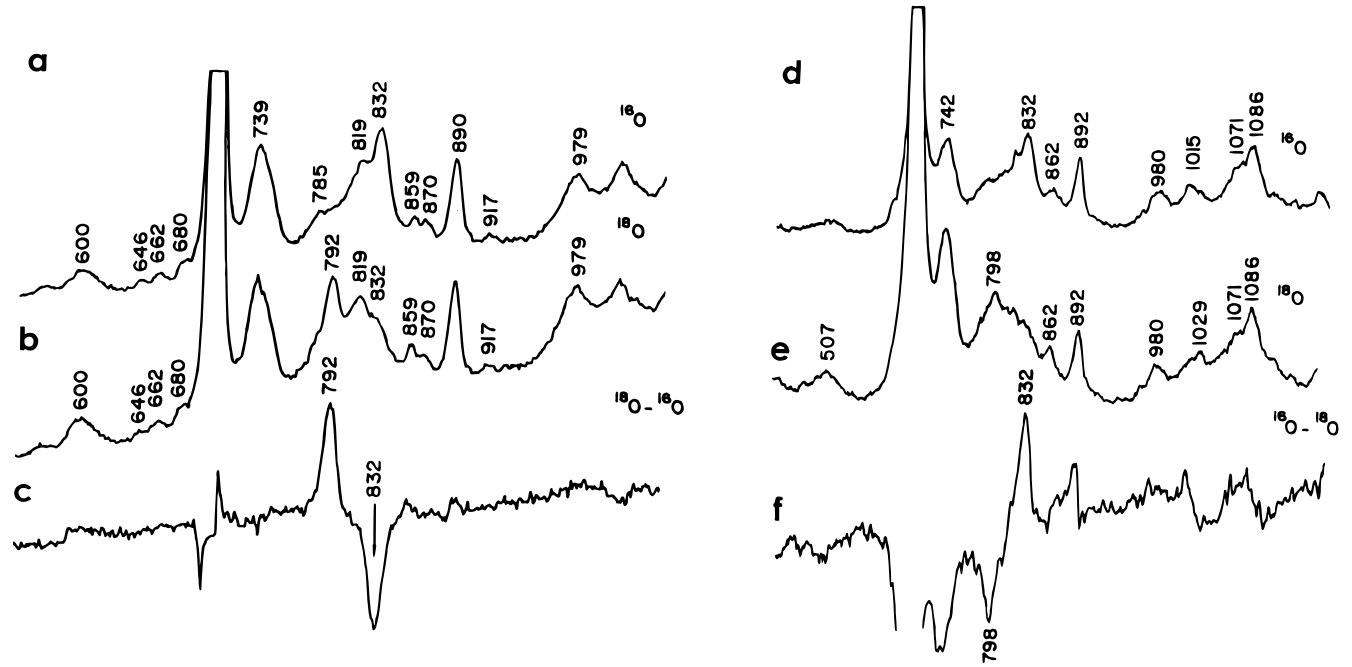

Figure 5. Resonance Raman spectra with 406.7 nm excitation (15 mW) for the 600−1000 cm^{-1} region at −80 °C for (a) (tetrakis(2,6-dichlorophenyl)-porphinato)iron(III) triflate in methylene chloride reacted with *m*CPBA and (b) reacted with ^{18}O-labeled *m*CPBA and (c) the difference spectrum b − a, identifying the $\nu_{Fe=O}$ of the (oxoferryl)porphyrin π-cation radical. Traces d−f show the corresponding data for the complex of 5-(2-chloro-6-nitrophenyl)-10,15,20-tris(2,6-dichlorophenyl)porphyrin.

interpreted in terms of the symmetry of the half-occupied porphyrin molecular orbital.[18,26] Of particular interest is the ν_2 mode, which has a strong pyrrole $C_\beta-C_\beta$ stretching component. The utility of ν_2 as a marker is in part derived from its A_{1g} symmetry (in D_{4h} notation) which allows its identification as a polarized band with substantial intensity under Soret excitation. The frequency shift of ν_2 upon oxidation of the porphyrin ring to a π-cation radical is a function of the nodal structure of the

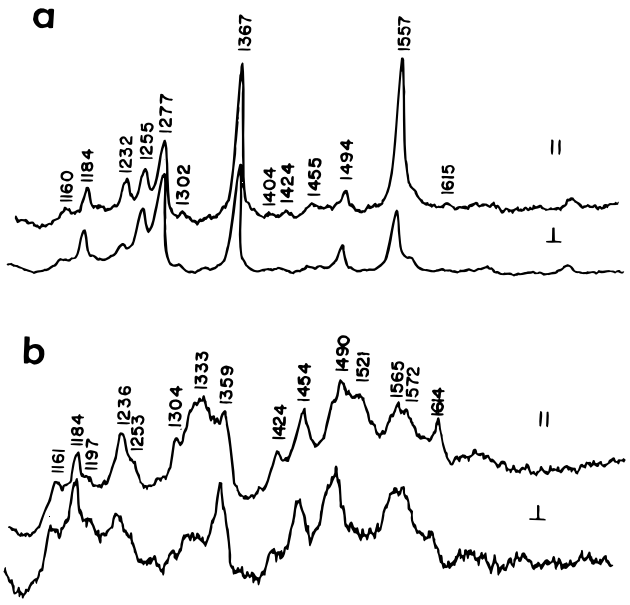

Figure 6. Resonance Raman spectra with 406.7 nm excitation (15 mW) for the 1250−1600 cm^{-1} region at −80 °C for (a) (tetramesitylporphinato)iron(III) chloride and (b) same compound as in part a but reacted with an 8-fold molar excess of *m*CPBA in methanol-d_4 forming the (oxoferryl)porphyrin π-cation radical.

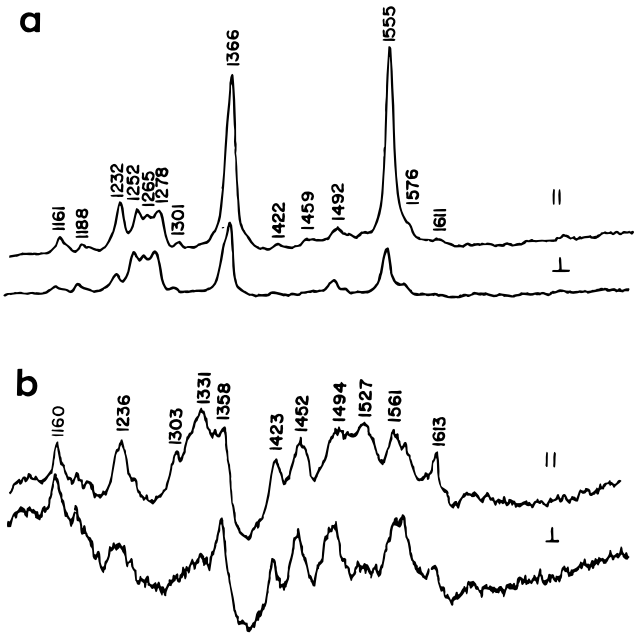

Figure 7. Resonance Raman spectra as in Figure 6, except with complexes of 2-iodotetramesitylporphyrin.

singly occupied molecular orbital[25,26] (a_{1u} or a_{2u} in D_{4h} notation) and is considered to be an identifier of electronic symmetry state. The a_{1u} orbital contains a node between the pyrrole β carbons, giving rise to an antibonding contribution to the $C_\beta-C_\beta$ bond energy. Since removal of an electron from the a_{1u} molecular orbital decreases the antibonding contribution, ν_2 is expected to upshift on porphyrin oxidation reflecting an increase in the $C_\beta-C_\beta$ bond strength. Conversely, the $C_\beta-C_\beta$ interaction in the a_{2u} molecular orbital is bonding. Abstraction of an electron from this molecular orbital results in bond weakening and a downshift of ν_2. These expectations are consistent with experimental observations[18,19,25] and are supported by MNDO calculations.[25] For octaethyl and tetraphenylporphyrin model compounds, which are close to idealized D_{4h} symmetry and represent prototypical a_{1u} and a_{2u} radicals respectively, ν_2 shifts up or down ≥ 30 cm^{-1}.

Table 6. Resonance Raman Frequencies (cm^{-1}) of Skeletal Modes of Iron Complexes of Tetramesitylporphyrin

mode	p	iron(III) chloro	$[Fe^{IV}=O(P)]^+$
ν_{phenyl}	p	1615	1614
ν_{10}	dp	1577	1572
ν_{37}			1565
ν_2	p	1557	1521
ν_{11}	dp	1494	1490
ν_{28}	dp	1470	1454
ν_3	p	1455	
CH_2Cl_2	dp	1424	1424
ν_{29}	dp	1371	1359
ν_4	p	1367	1333
ν_{12}	dp	1277	
	dp	1255	
ν_1	p	1232	1236
ν_{34}	dp	1184	1184
CH_2Cl_2	dp	1160	1161

Table 7. Resonance Raman Frequencies (cm^{-1}) of Skeletal Modes of Iron Complexes of 2-Iodotetramesitylporphyrin

mode	p	iron(III) chloro	$[Fe^{IV}=O(P)]^+$
ν_{phenyl}	p	1611	1613
ν_{10}	dp	1576	1576
ν_{37}	p		1561
ν_2	p	1555	1527
ν_{11}	dp	1492	1494
ν_{28}	dp		1452
ν_3	p	1459	
CH_2Cl_2	dp	1422	1423
ν_4	p	1366	1331
ν_{29}	dp	1366	1358
ν_{12}	dp	1278	
	dp	1265	
	dp	1252	
ν_1	p	1232	1236
ν_{34}	dp	1188	
CH_2Cl_2	dp	1161	1160

Following an approach used in correlating electronic state with marker band frequency shifts for the oxidation of (VO)-OEP and (VO)TPP to the corresponding porphyrin π-cation radicals,[26] band frequencies of the neutral oxoferryl complexes should be reference points for estimating band shifts on oxidation of the porphyrin ligands to form compound I analogs. This was done in the case of **1** and **2**; however, the spectrum of the oxoferryl complex of **3** was difficult to resolve because of fluorescence interference. Nevertheless, comparison of the resonance Raman spectra of the ferric and oxoferryl complexes of **1** and **2**, shows that the differences in marker band positions for coordination of a neutral porphyrin either to a high-spin ferric ion or to an oxoferryl unit are small. Therefore, the ferric spectrum was used as a reference for evaluating shifts of the porphyrin normal modes on oxidation of **3** to the (oxoferryl)-porphyrin π-cation radical.

Molecular orbital calculations place the energy of the a_{2u} orbital of *meso*-tetraarylporphyrins slightly above that of the a_{1u} orbital,[22,41] making A_{2u} the expected ground state of the tetraarylporphyrin π-cation radicals. However, changing the electronic character of peripheral substituents is predicted to alter the energy gap between the a_{2u} and a_{1u} frontier orbitals.[22] Because of the large atomic orbital coefficient of the a_{2u} molecular orbital at C_m, substitution at porphyrin *meso* carbons is expected to exert a pronounced influence on $a_{1u}-a_{2u}$ separation. Electron-withdrawing *meso* substituents stabilize the a_{2u} molecular orbital, and highly electronegative *meso* groups such as cyanide are predicted to favor electron abstraction from the a_{1u} orbital. Ferric TMP, with electron-releasing *meso* substit-

(41) Loew, G. H.; Axe, F. U.; Collins, J. R.; Du, P. *Inorg. Chem.* **1991**, *30*, 2291−2294.

uents, has been shown to form a compound I analog having the expected a_{2u} symmetry by the ν_2 band-shift criterion. The 36 cm^{-1} downshift observed for ν_2 in this study is identical to that reported by other workers.[8−10] Ferric 2-iodoTMP, which also has electron releasing *meso* substituents, shows a 28 cm^{-1} downshift in ν_2 on oxidation to the compound I analog (Figure 7, Table 7).

The behavior of the ν_2 mode of the compound I analogs of **1**−**3** differs significantly from that observed for the oxidized TMP and 2-iodoTMP complexes, as well as other *meso* tetraaryl porphyrin π-cation radicals considered to have a_{2u} symmetry.[18,25,42] In contrast to a large expected downshift, we note no significant shift of ν_2 in the resonance Raman spectra of the compound I analogs of **1**−**3** relative to its position in complexes of the neutral porphyrin ligands (compound II analogs or ferric complexes).

$C_\beta-C_\beta$ stretching is also a major component of ν_{11}, which is therefore expected to parallel the behavior of ν_2 in the compound I analogs.[25,36] MNDO calculations predict that ν_{11} will exhibit large up- or downshifts (approximately 20 cm^{-1}) upon formation of an a_{1u} or a_{2u} radical cation, respectively. Though easily detected in neutral porphyrins, ν_{11} is not always readily identifiable in the radical cations. However, ν_{11} has been identified in the (oxoferryl)porphyrin π-cation radical complexes of **1** and **2**, as well as in the complexes of the neutral porphyrins, and shifts up by ∼15 cm^{-1} on porphyrin oxidation. Shifts of ν_{11} observed for a_{2u} *meso* tetraarylporphyrin[25] π-cation radicals have sometimes been small (5 cm^{-1}). For TMP and 2-iodoTMP, ν_{11} shifts by only a few wave numbers in the compound I analogs. Thus, behavior of the marker band ν_{11} in compound I analogs of **1** and **2** contrasts with that observed for the compound I analogs of TMP and 2-iodoTMP, which have a_{2u} symmetry.

The porphyrin mode ν_4, composed primarily of $C_\alpha-N$ and $C_\alpha-C_\beta$ stretching, has also been examined as an indicator of symmetry state of porphyrin π-cation radicals.[25] Despite predicted upshifts for a_{2u} radicals and downshifts for a_{1u} radicals, downshifts have been experimentally observed in all cases for both a_{1u} and a_{2u} π-cation radicals.[18,25,26,42] The ν_4 mode shifts downward in all of the compound I analogs investigated in this study. However, we do observe a larger downshift for the (oxoferryl)porphyrin π-cation radicals generated from **1**−**3** than for the a_{2u} complexes generated from TMP or 2-iodoTMP. A similar trend is reported for the shift of ν_4 in a_{1u} porphyrin π-cation radicals relative to a_{2u} porphyrin π-cation radicals.[25,26]

The marker bands of complexes **1**−**3** behave in a distinctly different fashion from the marker bands of the complexes of TMP and 2-iodoTMP on generation of the compound I analogs. It is unlikely that these differences simply reflect small structural effects of the substituents. The frequencies of ν_2 and ν_{11}, the modes of primary interest as symmetry state indicators, appear within a 5 cm^{-1} window for the ferric complexes of neutral **1**−**3**, TMP, and 2-iodoTMP. The ν_2 band of the oxidized 2-iodoTMP complex, in which the bulky peripheral iodine substituent removes 4-fold symmetry, behaves as predicted for an a_{2u} π-cation radical. Ruffling has been shown not to alter $C_\beta-C_\beta$ energies,[43] while significant saddle distortion causes large *down*shifts[38,39] of ν_2. In addition, severe saddle distortion would be reflected in a large red-shift of the visible band in the electronic spectrum of the π-cation radicals,[44] and such a shift is not observed in the spectra of compound I analogs of **1**−**3** or 2-iodoTMP. The behavior of ν_2 and ν_{11} implies that the $C_\beta-C_\beta$ bonds in the oxidized complexes of **1**−**3** have not been substantially weakened by electron abstraction from the porphyrin ligand. This situation is consistent with relatively decreased $C_\beta-C_\beta$ antibonding interactions that would arise from admixture of a_{1u} character into the half-occupied molecular orbital of the porphyrin π-cation radical. Such a determination is in accord with conclusions based on an ^1H NMR study of several compound I analogs,[11] including complex **1**. Resonance Raman spectroscopy has, in fact, been suggested[11] as an independent test of this hypothesis, and the results of this study provide support for such an admixture.

In the low-frequency region, an up- or downshift of $\nu_{Fe=O}$ relative to the neutral oxoferryl complex has also been suggested as indicative of symmetry state. The proposed correlation is based upon orbital mixing arguments used to explain the shift of $\nu_{V=O}$ observed on oxidation of oxovanadium octaethylporphyrin to an a_{1u} cation radical (upshift) and oxovanadium *meso*-tetraphenylporphyrin to an a_{2u} cation radical (downshift).[26] However the applicability of this correlation to iron porphyrin complexes has yet to be fully explored. A study has compared[10] the resonance Raman spectra of (oxoferryl)porphyrin π-cation radicals generated from octaethylporphyrin, *meso*-tetraphenylporphyrin, and *meso*-tetramesitylporphyrin complexes in a solid O_2 matrix under identical conditions. Although these macrocycles are expected to effect the symmetry state of the porphyrin π-cation radical,[18] downfrequency shifts of $\nu_{Fe=O}$ relative to the neutral oxoferryl complexes were observed for all the (oxoferryl)porphyrin π-cation radicals. In the case of (oxoferryl)porphyrin π-cation radicals generated in solution, complications in correlating $\nu_{Fe=O}$ with symmetry state are introduced by both solvent effects and the presence of axially ligating species in the reaction mixtures.[8] For oxidation of complexes **1**−**3**, methanol is required in the reaction mixtures in order to obtain quantitative conversion to the compound I analogs. It is possible that the downfrequency shift superimposed by methanol coordination *trans* to the oxo oxygen ligand[8] would mask effects of the porphyrin π-cation radical symmetry state.

The observation here and in ref 10 that $\nu_{Fe=O}$ is not sensitive to peripheral substituents is relevant to the function of compound I analogs in biomimetic monooxygen transfer reactions. The implied constancy of iron−oxygen bond strength over a range of electron-withdrawing and electron-releasing *meso* substituents supports the suggestion[11] that reactivity of compound I analogs in epoxidation of olefins may be attributed to differences in porphyrin oxidation potential.

The large upfield NMR hyperfine shifts of the pyrrole protons and aryl *m*-protons of the compound I analogs on changing the *meso* aryl substituents from electron-releasing in TMP to electron-withdrawing in **1** have been reported previously and explained by a_{2u}/a_{1u} symmetry state admixing.[11] The hyperfine NMR shifts observed in this study for the oxidized complexes of **1** and TMP are identical to those reported in ref 11. The hyperfine proton shifts of the compound I analogs generated from **2** and **3** are consistent with an unpaired electron spin density distribution similar to that observed for the π-cation radical of **1** (Figure 2), while those of the compound I analog generated from 2-iodoTMP are consistent with the unpaired electron spin density distribution of an a_{2u} π-cation radical, as observed for TMP (Table 2).

UV−visible and Mössbauer spectroscopy were useful in the optimization of conditions for generating (oxoferryl)porphyrin π-cation radicals cleanly and in high yield, since these techniques are sensitive to ferric and ferryl contaminants under the

(42) Kitagawa, T.; Mizutani, Y. *Coord. Chem. Rev.* **1994**, *135/136*, 685−735.
(43) Alden, R. G.; Crawford, B. A.; Doolen, R.; Ondrias, M. R.; Shelnutt, J. A. *J. Am. Chem. Soc.* **1989**, *111*, 2070−2072.
(44) Ochsenbein, P.; Mandon, D.; Fischer, J.; Weiss, R.; Austin, R.; Jayaraj, K.; Gold, A; Terner, J.; Bill, E.; Müther, M.; Trautwein, A. X. *Angew. Chem., Int. Ed. Engl.* **1993**, *32*, 1437−1439.

oxidation conditions. As further evidence of the efficiency of the oxidations, the iron spins initially present in EPR sample solutions of high-spin ferric starting compounds were accounted for by quantitation of the electron spins of the EPR-active spin quartets of the compound I analogs. Isomer shifts and hyperfine magnetic coupling observed in the Mössbauer spectra confirm the presence of both ferryl iron and the porphyrin radical in the oxidized species and rule out the possible structural assignment of high-spin Fe(V)[45,46] coordinated to a neutral porphyrin ligand. Simulation of EPR and Mössbauer spectra assure that the qualitative behavior of all the compound I analogs in this study conforms to the general description of parallel-coupled (oxoferryl)porphyrin π-cation radicals. EPR and Mössbauer studies of a number of compound I analogs, including 2-iodoTMP,[33] indicate that symmetry perturbations at the porphyrin periphery are not readily communicated to iron. On the basis of this finding, the observation of parallel coupling in all of the compound I analogs investigated in this study is predictable. Recent calculations showing significant unpaired spin on pyrrole nitrogens, even for "pure" a_{1u} π-cation radicals,[25] suggest that spectroscopic measurements such as EPR and Mössbauer, which are dependent on delocalized molecular interactions, may not be sensitive functions of admixing of symmetry states.

(45) Nanthakumar, A.; Goff, H. M. *J. Am. Chem. Soc.* **1990**, *112*, 4047−4049.
(46) Yamaguchi, K.; Watanabe, Y.; Morishima, I. J. *Chem. Soc., Chem. Commun.* **1992**, 1721−1723.

Conclusion

(Oxoferryl)-*meso*-tetraarylporphyrin π-cation radicals, generated from a series of complexes **1**−**3** in which the substituents are highly electron-withdrawing, were compared to the tetramesityl and 2-iodotetramesityl complexes in which the *meso*-aryl groups are electron-releasing. Of particular interest in the resonance Raman spectra was the behavior of skeletal modes ν_2 and ν_{11}, considered to be indicators of electronic symmetry state of the porphyrin π-cation radical. The shifts observed for these marker bands on oxidation of the ferric complexes to compound I analogs support the proposal of substituent-mediated admixture of a_{1u} character into the a_{2u} ground state of the *meso*-tetraaryl compound I analogs. The Fe═O stretch of the compound I analogs of **1**−**3** and TMP appears at the same frequency under identical experimental conditions, suggesting that the strength of Fe═O bonding is not highly sensitive to the nature of peripheral substituents in (oxoferryl)porphyrin π-cation radicals.

Acknowledgment. This work was supported in part by USPHS Grants GM34443 (J.T.) and ES03433 (A.G.), Centre National de la Recherche Scientifique Grant UA424 (R.W.), and the Deutsche Forschungsgemeinschaft (A.X.T.). A.G. thanks the NSF for Grant INT-9314422, and A.G. and R.W. also thank NATO for collaborative research grants. We are indebted to J. Antoni and M. Grodzicki for many fruitful discussions.

IC951058V